Proceedings of the 2012 IEEE 12th International Conference on Bioinformatics & Bioengineering (BIBE), Larnaca, Cyprus, 11-13 November 2012

Head Posture Influences the Geometric and Hemodynamic Features on the Healthy Human Carotid Bifurcation

Nicolas Aristokleous[1], Ioannis Seimenis[2], Yannis Papaharilaou[3], Mohammad Iman Khozeymeh[1], Georgios C. Georgiou[4], Brigitta C. Brott[5], Andreas S. Anayiotos[1]

[1]Dept. of Mech. Eng. and Materials Science and Eng., Cyprus University of Technology, Limassol, Cyprus

[2]Department of Medicine, Democritus University of Thrace, Alexandroupolis, Greece

[3]Institute of Applied and Computational Mathematics, Foundation for Research and Technology-Hellas, Heraklion, Creten, Greece

[4]Department of Mathematics and Statistics, University of Cyprus, Nicosia, Cyprus

[5]Department of Medicine, University of Alabama at Birmingham, Birmingham, USA

Abstract— **Atherosclerosis is the third leading cause of morbidity and mortality in the Western world. Low and oscillating wall shear stress (WSS) regions have been previously reported as parameters that correlate with the development of atherosclerosis. In this study we investigated geometric and hemodynamic changes in the carotid bifurcation as a result of posture change. Data from magnetic resonance imaging (MRI) were used to construct three dimensional (3D) surface models and computational fluid dynamic (CFD) fields. Two healthy volunteers were imaged by MRI in three different head postures: a) the supine neutral (N) head position, b) the prone position with leftward head rotation (LR) up to 80^o and c) the prone position with rightward head rotation (RR) up to 80^o. The area exposure to unfavorable hemodynamics, based on thresholds set for oscillatory shear index (OSI), WSS and relative residence times (RRT), was used to quantify the hemodynamic impact on the wall. Significant change in the hemodynamic burden on the wall was found for the OSI. The velocity profile at the common carotid artery (CCA) upstream of the carotid bifurcation (CB) was investigated at the supine and RR prone position for six healthy volunteers. The results indicated that blood flow rate decreased at peak systole, for the prone position for both the right and left CCAs.**

Keywords-Image-based CFD; Wall shear stress; Posture change; Geometry characterisation; Atherosclerosis

I. Introduction

Cardiovascular disease continues to be the principal cause of death in United States, Europe and much of Asia [1], and research over the last few decades shows that vessel geometry and hemodynamic forces influence the vascular pathology. Regions of disturbed flow, like bifurcations, have increased chances of atheroma deposition [2]. Previous studies have shown that posture changes may influence the geometry of the carotid bifurcation and consequently alter hemodynamics [3,4].

The employment of imaging techniques such as MRI allows for the construction of realistic 3D surface arterial models from anatomical images with patient specific geometric characteristics and provides boundary conditions for the reconstruction of CB hemodynamics with CFD [5,6]. Recent studies with large number of participants report the feasibility and reliability in reproducing the CB geometry with routine contrast enhanced MR angiography [7].

This study aims to assess the geometric changes and the corresponding hemodynamic changes associated with bilateral head rotation in two healthy volunteers. Using phae-contrast MRI, we also studied the blood flow field at a location of CCA around 20mm below CB for six healthy subjects. The measurements were performed for the right and left CCA at the supine neutral head position and at prone position with RR head rotation.

II. Materials and Methods

A. Study Group

Two healthy male volunteers (31 and 33 years) participated in the bilateral geometry and CFD study. For the blood velocity measurements, four more healthy men were added in the group of volunteers (n=6, mean age of 30 years

range 22 to 39 years). The study was approved by the Cyprus Bioethics committee (2011).

B. MR Imaging

MR images were acquired using a 3T MRI instrument (Achieva, Philips Medical Systems, the Netherlands). Regarding the morphological study, each subject was imaged in three different scanning sessions corresponding to the three investigated head postures: a) the supine neutral (N) head position, b) the prone position with leftward head rotation (LR) up to 80^o and c) the prone position with rightward head rotation (RR) up to 80^o. Regarding the blood flow study, two scans were performed corresponding to the N and RR head postures. Anatomical data were obtained with a time-of-flight (TOF) method employing a 3D gradient-echo pulse sequence (echo time (TE)=3.5ms, repetition time (TR)=23ms, a flip angle (FA)=20°, 0.36x0.36x1.2mm^3 acquisition voxel and 0.2x0.2x.0.6 mm^3 reconstruction voxel). A peripheral pulse triggered 2D phase sensitive pulse sequence was employed to acquire flow data spread in 20 phases over the cardiac cycle.

C. Surface Reconstruction and Geometric Feature Quantification

The solid surface models were constructed by slice-by-slice manual segmentation using the ITK-Snap software (PICSL, USA) [8] and various features of the vascular modeling toolkit (VMTK) [9]. Specific important geometric parameters, such as bifurcation angle, ICA angle, ICA planarity angle, in-plane asymmetry angle, curvature, tortuosity, bifurcation area ratio, and diameter ratios were identified and determined according to relevant published definitions [4, 10].

D. Carotid Artery Blood Flow

Blood flow data were acquired at a distance approximately 3 diameters away the flow divider (~20 mm) for both the left and right CCAs,. The blood velocity was obtained at each pixel and then the blood velocity waveform was calculated for each vessel. From those waveforms we were able to estimate the maximum systolic velocity (V_{peak}), the peak velocity averaged over one cardiac cycle (V_{cyc}) and the mean blood flow (Q_{cyc}). The velocity calculation from MR images was done using ImageJ (ImageJ, NIH, USA).

E. CFD Method

To investigate the blood flow for the two healthy volunteers, the computational domain for CB surfaces obtained by MR images was spatially discretized with ICEM-CFD v12.1 (Ansys Inc.) using ~$8.5 \cdot 10^5$ mixed type elements with higher grid density in the vicinity of the CB and a viscous layer adjacent to the wall. The Navier-Stokes equations were solved numerically using Fluent v12.1 (Ansys Inc.). The vessel wall was assumed to be rigid and blood was modeled as an incompressible Newtonian fluid with a density of 1.05gr cm^3 and a viscosity of 3.5 cP. A physiological CCA flow waveform from a healthy male volunteer was used for all cases, to prescribe the inlet boundary condition and a constant 0.65/0.35 (ICA/ECA) flow split was applied. The spatiotemporally averaged Reynolds number was Re_m=305 at the inlet and the Womersley parameter was α=4.0. A second-order upwind discretisation scheme was applied for the momentum equations and a 2 -order interpolation scheme for the pressure. The PISO algorithm was used for pressure velocity coupling. A time periodic solution was achieved after 3 flow cycles. A systematic time-step and grid size independence study was carried out, which indicated that a time step of Δt =6.5 10^{-6} normalized by the spatiotemporal mean inlet velocity per inlet diameter which resulted in 4000 time steps per flow cycle. Then, the following hemodynamic parameters were calculated: a) the OSI with the range of values 0<OSI<0.5, where 0 corresponds to unidirectional shear flow and 0.5 to the purely oscillatory shear case; b) the normalized OSI (nOSI), which is calculated by dividing the OSI by the time averaged WSS (TAWSS) magnitude normalized by the time averaged inlet Poiseuille flow WSS and shows the regions of low and oscillatory shear; c) the WSSTG, also calculated at each time step; and finally d) the computed relative residence time (RRT).

III. Results

Figure 1 shows the magnitude image and the phase-contrast image 3 inlet diameters upstream of the CB flow divider.

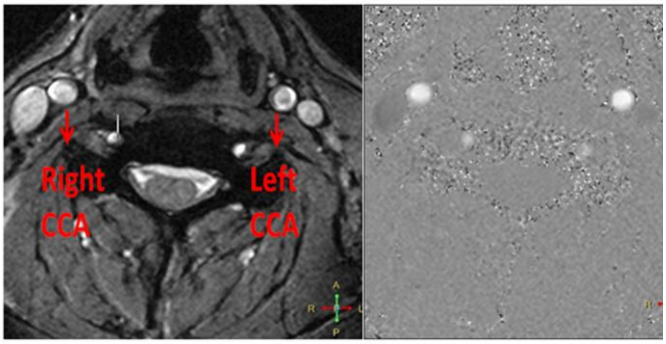

Figure 1: Magnitude image (left) and phase-contrast image (right) at the level of 3D (~20 mm) below CB.

Figure 2 represents the color map at peak systole for the right and left CCAs for both volunteers and the two investigated head postures.

Figure 3 shows the mean blood flow from all six volunteers averaged over the whole cross section for the right and left CCAs and for the two head postures.

Figure 4 shows the comparison between the neutral and prone position averaged velocity profiles along the vertical and horizontal diameter positions. This was done by calculating the average velocity in several points along the two diameters over the 20 phases of the cardiac cycle for the 6 volunteers.

Table I shows the peak velocities and flow rates in the neutral and rotated head postures for both carotids from the 6 volunteers of this study and from healthy??? volunteers of other studies.

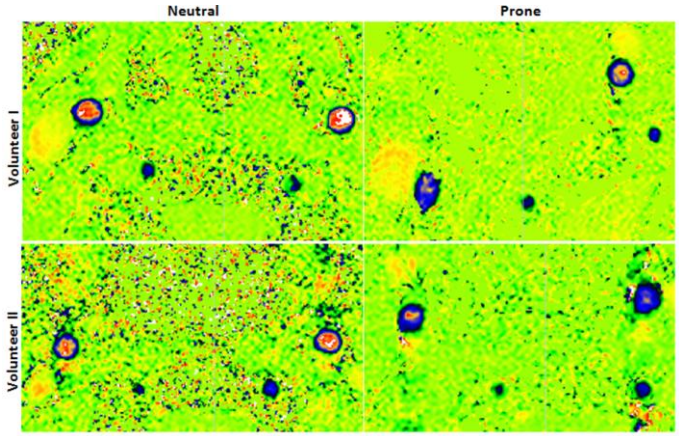

Figure 2: Velocity color map at the peak systole for the axial plane 3D below CB for both carotids for the two head postures and the two volunteers (black color for minimum velocity and white for maximum).

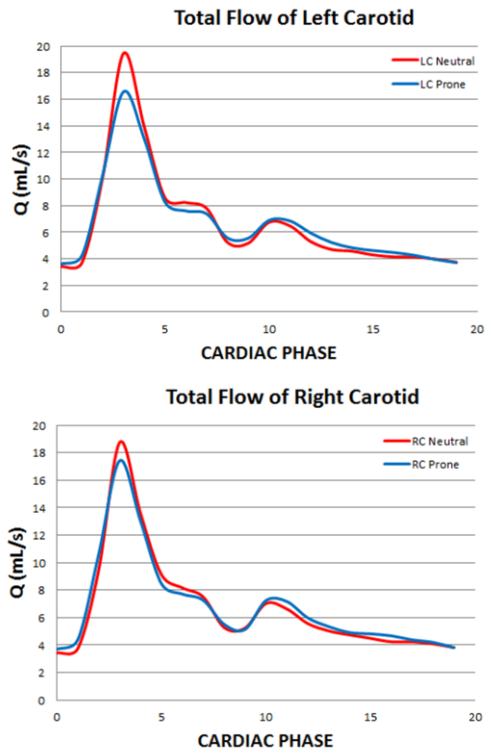

Figure 3: Total blood flow from all volunteers (n=6) for the two investigated head postures

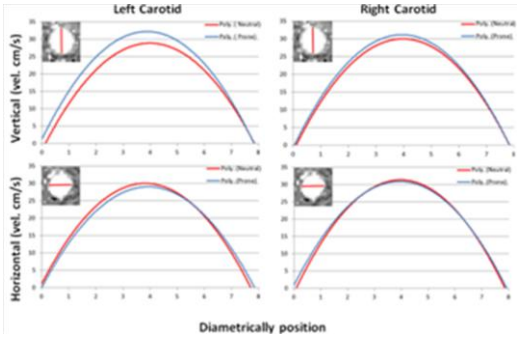

Figure 4: Comparison between Neutral and Prone position velocity profiles along vertical and horizontal diameter positions.

TABLE I. BLOOD FLOW PARAMETERS FOR THESIX VOLUNTEERS AND MEASUREMENTS FROM PREVIOUS STUDIES

	Head Posture	n=6		Mean	Studies	
	Carotid	RC	LC			
Blood Flow ($Q_{cyc,}$ mL/s)	neutral	6.7	6.7	6.7	6[11]	6.5[12]
	prone	6.8	6.7	6.8	-	-
Blood Velocity ($V_{peak,}$ cm/s)	neutral	37.1	37.3	37.2	38.8[11]	40.9[13]
	prone	37.7	33.9	35.8	-	-
V peak max	neutral	81.8	83.6	83	108.2[11]	77.5[12]
	prone	84.5	72.8	78.7	-	-

[11]Holdsworth et al (n=17), [12]Vannimen et al (n=10), [13]Schoning et al (n=48)

The influence of the morphology changes observed in the 3D surface models on the computed flow field is qualitatively depicted in Figs. 5 and 6.

Figure 5 shows the contour plots of time-averaged nOSI and WSSTG for right and left CB in the 3 investigated postures

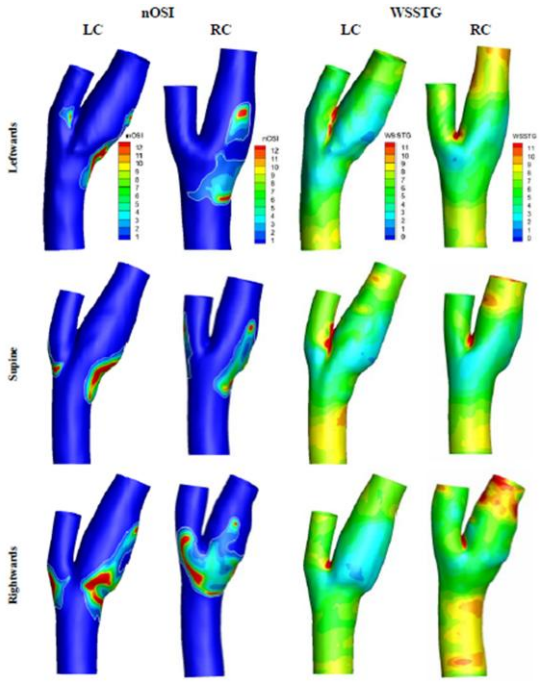

Figure 5: represents the contour plots of time-averaged nOSI and WSSTG for right and left CB in the 3 investigated postures.

Figure 6 shows the contour plots of time-averaged OSI and RRT for right and left CB in the 3 investigated postures.

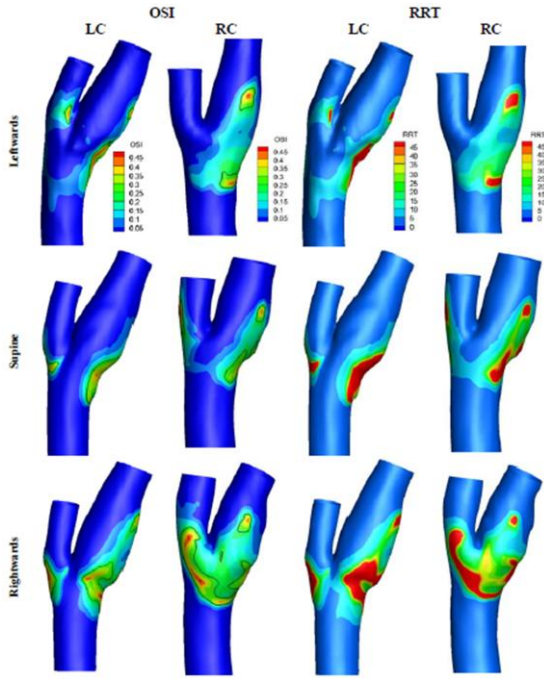

Figure 6: contour plots of time-averaged OSI and RRT for right and left CB in the 3 investigated postures.

Table II summarizes the changes in the bifurcation and ICA angles due to head rotation. In most but not all cases, cross sectional area ratios for CCA, ICA and ECA change due to head posture change.

TABLE II. GEOMETRIC PARAMETERS FOR THE THREE DIFFERENT HEAD POSTURES

Geometric Parameter			Volunteer I		Volunteer II	
			LC	RC	LC	RC
Angles (degrees)	Bifurcation Angle	LR-N	-6.3±0.54	3.4±0.54	-7.7±0.54	9.5±0.54
		N	54.65	40.74	45.34	31.09
		RR-N	-23.6±0.54	16.8±0.54	-5.7±0.54	15.3±0.54
	ICA Angle	LR-N	-2.1±1.19	3.5±1.19	-9.17±1.19	17.9±1.19
		N	26.3	22.73	28.88	15.73
		RR-N	-18.4±1.19	12.7±1.19	-16.2±1.19	13.2±1.19
Area Ratios	Bif. Area Ratio $(ICA_5+ECA_5)/CCA_3$	LR-N	-0.03±0.06	-0.15±0.06	0.13±0.06	0.35±0.06
		N	1.21	1.34	1.14	1.0
		RR-N	0.27±0.06	-0.11±0.06	0.03±0.06	0.21±0.06
	ICA_5/CCA_3	LR-N	-0.07±0.02	0.08±0.02	-0.08±0.02	0.12±0.02
		N	0.82	0.76	0.85	0.77
		RR-N	-0.1±0.02	0.06±0.02	-0.04±0.02	0.12±0.02
	ECA_5/CCA_3	LR-N	0.04±0.03	-0.17±0.03	0.01±0.03	0.12±0.03
		N	0.74	0.87	0.64	0.63
		RR-N	-0.1±0.03	-0.12±0.03	0.03±0.03	0.01±0.03
	ECA_5/ICA_5	LR-N	-0.1±0.01	-0.1±0.01	0.1±0.01	0.03±0.01
		N	0.9	1.14	0.75	0.82
		RR-N	0.0±0.01	-0.22±0.01	0.07±0.01	-0.1±0.01

IV. Discussion

The results of this study indicate that torsion of the neck associated with head rotation may cause changes in the geometric and hemodynamic characteristics of the healthy carotid bifurcation in volunteers. Our earlier results for 10 healthy volunteers [4] and those of Glor et al. [6] for healthy volunteers have indicated differences in CB shape and hemodynamic features with respect to head rotation. This study confirms that thiese changes occur in both the right and left CB.

In addition, our present study has shown that blood flow rate and consequently the mean and maximum velocity at peak systole change with head rotation. This may be due to changes in the downstream impedance with head rotation. Velocity profiles along the vertical diameter also shows moderate alterations, probably due to head position changes. However, blood flow rate in the CCA seems to remain unaffected, possibly due to the combined effect of morphology and velocity changes.

For many individuals, there is a substantial time period with prolonged head rotation which occurs during sleep. This may provide a long enough duration of altered flow that may influence the process of atherosclerotic development and/or the conditions that may lead to the rupture of unstable plaque. It is also important to investigate the stress distributions for all possible postures, in order to optimize device placement and minimize the possibility of restenosis for implanted carotid stents.

Further studies and research however are warranted with more systematic clinical studies to evaluate the effect of head rotation on normal and on carotid stenotic CBs.

Acknowledgment

This work was co-funded by the European Regional Development Fund and the Republic of Cyprus through the Research Promotion Foundation (Project ΥΓΕΙΑ/ΔΥΓΕΙΑ/ 0609 (BIE)/11).

References

[1] R. Rosss, "Mechanism of Disease: Atherosclerois – An Inflammatory Disease," N. Engl. J. Med., vol. 340, pp. 115–126, Jan, 1999.

[2] I. Marshall, S. Zhao, P. Papathanasopoulou, P. Hoskins and Y. Xu, "MRI and CFD studies of pulsatile flow in healthy and stenosed carotid bifurcation models," J. Biomech., vol. 37, pp. 679-687, May, 2004.

[3] F. P. Glor, B. Ariff, A. D. Hughes, P. R. Verdonck, D. C. Barratt, A. D. Augst, S. A. Thom and X. Y. Xu, "Influence of head position on carotid hemodynamics in young adults," Am. J. Physiol. Heart Circ. Physiol., vol. 287, pp. H1670-81, Oct, 2004.

[4] N. Aristokleous, I. Seimenis, Y. Papaharilaou, G. C. Georgiou, B. C. Brott, E. Eracleous and A. S. Anayiotos, "Effect of posture change on the geometric features of the healthy carotid bifurcation," IEEE Trans. Inf. Technol. Biomed., vol. 15, pp. 148-154, Jan, 2011.

[5] D. A. Steinman, J. B. Thomas, H. M. Ladak, J. S. Milner, B. K. Rutt and J. D. Spence, "Reconstruction of carotid bifurcation hemodynamics and wall thickness using computational fluid dynamics and MRI," Magn. Reson. Med., vol. 47, pp. 149-159, Jan, 2002.

[6] F. P. Glor, Q. Long, A. D. Hughes, A. D. Augst, B. Ariff, S. A. Thom, P. R. Verdonck and X. Y. Xu, "Reproducibility study of magnetic

resonance image-based computational fluid dynamics prediction of carotid bifurcation flow," Ann. Biomed. Eng., vol. 31, pp. 142-151, Feb, 2003.

[7] P. B. Bijari, L. Antiga, B. A. Wasserman and D. A. Steinman, "Scan-Rescan reproducibility of carotid bifurcation geometry from routine contrast-enhanced MR angiography," J. Magn. Reson. Imaging, vol. 33, pp. 482-489, Feb, 2011.

[8] P. A. Yushkevich, J. Piven, H. C. Hazlett, R. G. Smith, S. Ho, J. C. Gee and G. Gerig, "User-guided 3D active contour segmentation of anatomical structures: Significantly improved efficiency and reliability," Neuroimage, vol. 31, pp. 1116-1128, 2006.

[9] L. Antiga and D. A. Steinman, "Robust and objective decomposition and mapping of bifurcating vessels," IEEE Trans. Med. Imaging, vol. 23, pp. 704-713, Jun, 2004.

[10] J. B. Thomas, L. Antiga, S. L. Che, J. S. Milner, D. A. Steinman, J. D. Spence, B. K. Rutt and D. A. Steinman, "Variation in the carotid bifurcation geometry of young versus older adults: implications for geometric risk of atherosclerosis," Stroke, vol. 36, pp. 2450-2456, Nov, 2005.

[11] D. W. Holdsworth, C. J. Norley, R. Frayne, D. A. Steinman and B. K. Rutt, "Characterization of common carotid artery blood-flow waveforms in normal human subjects," Physiol. Meas., vol. 20, pp. 219-240, Aug, 1999.

[12] R. L. Vanninen, H. I. Manninen, P. L. Partanen, P. A. Vainio and S. Soimakallio, "Carotid artery stenosis: clinical efficacy of MR phase-contrast flow quantification as an adjunct to MR angiography," Radiology, vol. 194, pp. 459-467, Feb, 1995.

[13] M. Schoning, J. Walter and P. Scheel, "Estimation of cerebral blood flow through color duplex sonography of the carotid and vertebral arteries in healthy adults," Stroke, vol. 25, pp. 17-22, Jan, 1994.